

# Low temperature thermal properties of Nafion 117 membranes in water and methanol-water mixtures

Horacio R. Corti<sup>a,b,\*</sup>, Federico Nores-Pondal<sup>a,b</sup>, M. Pilar Buera<sup>b,c</sup>

<sup>a</sup> *Unidad de Actividad Química, Centro Atómico Constituyentes, Comisión Nacional de Energía Atómica, Av. General Paz 1499 (1650) San Martín, Buenos Aires, Argentina*

<sup>b</sup> *Consejo Nacional de Investigaciones Científicas y Técnicas, Buenos Aires, Argentina*

<sup>c</sup> *Departamento de Industrias, Facultad de Ciencias Exactas y Naturales, Universidad de Buenos Aires, Av. Cantillo s/n, Ciudad Universitaria (1428), Buenos Aires, Argentina*

Received 27 March 2006; received in revised form 21 May 2006; accepted 6 June 2006

Available online 12 July 2006

## Abstract

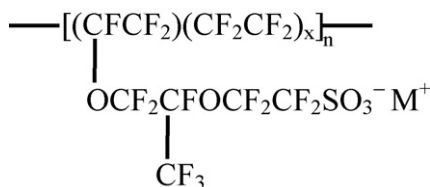
The low temperature thermal behavior of Nafion 117 membranes with different water contents and equilibrated with water–methanol mixtures of different concentrations were studied by differential scanning calorimetry (DSC). The DSC curves revealed a weak transition at temperatures below  $-100^{\circ}\text{C}$ , related to the  $\gamma$  peak reported in mechanical dynamics studies, and associated to the true glass transition temperature of the polymer. The amount of freezable water was determined from the area of the ice fusion peak and it increased from 1 to 23% as the relative humidity increases from 84 to 100%. The presence of methanol in the membrane increased the amount of freezable water up to 65%.

© 2006 Elsevier B.V. All rights reserved.

**Keywords:** Nafion; DMPEM fuel cells; Glass transition temperature; Water; Methanol; Freezing

## 1. Introduction

Nafion 117 is a perfluorosulfonated ionomer that possesses high chemical, mechanical and thermal stability, due to its polytetrafluoroethylene (PTFE) backbone with perfluoroalkylethersulfonate side chains. The structure of commercially available Nafion-117 membrane is shown below [1], where  $x=6.5$ , and  $\text{M}^+$  is an exchangeable counterion with a capacity (dry) of  $0.91 \text{ meq g}^{-1}$  (equivalent weight = 1100).



It is used mainly as electrolyte membrane in hydrogen feed proton exchange membrane (PEM) fuel cells and in chlorine-

alkali cells for the production of chlorine and caustic soda [2]. Direct methanol PEM fuel cells (DMPEM) feed with liquid methanol also use Nafion as electrolyte, but a number of alternative ionomeric materials are being tested to overcome the methanol crossover problem associated with the high permeability of methanol through Nafion. The detailed characterization of Nafion membrane is essential for the development of its technological applications.

The sorption behavior of Nafion in water and methanol has been reported by several authors [3–6]. At ambient conditions, the maximum values for water and methanol uptake by immersion of the membrane in the corresponding liquid are  $0.220 \text{ g g}^{-1}$  dry membrane and  $0.492 \text{ g g}^{-1}$  dry membrane, respectively [3]. The transport ions [7–12], water [7,10,12–16], and methanol [9,10,12,17,18] in Nafion membranes has also been studied as a function of the solvent content and temperature.

In a recent comprehensive review on the properties of Nafion, Mauritz and Moore [19] describes the state of the art regarding the morphological characterization of Nafion. The X-ray and neutron scattering experiments are discussed and the models of Nafion structure are analyzed in detail as well as the molecular

\* Corresponding author. Tel.: +54 11 6772 7174; fax: +54 11 6772 7886.  
E-mail address: [hrcorti@cnea.gov.ar](mailto:hrcorti@cnea.gov.ar) (H.R. Corti).

dynamics simulation of the membrane structure and its mechanical properties. After reviewing the dynamics mechanical properties of Nafion these authors concluded that the differences in the assignment of the glass transition temperature  $T_g$  of the matrix was confusing.

The vast information on the structure of Nafion can be summarized as follow [19]: the ionomer morphology reorganizes as the dry membrane is swollen with water. The dry state correspond to isolated spherical ionic clusters with diameters of around 1.5 nm dispersed in a perfluorinated matrix. With the uptake of water the clusters start to hydrate and their diameters increase up to 4 nm forming “nano-pools” of water surrounded by ionic  $-\text{SO}_3^-$  groups, connected each other by channels of diameter smaller than the clusters.

Because this work is devoted mainly to the analysis of the different thermal relaxations of Nafion membranes containing water and methanol in the next subsections we briefly review the mechanical (based on the review by Mauritz and Moore [19]) and thermal properties of this material.

### 1.1. Dynamics mechanical properties

The first torsional pendulum studies performed on the acid form of Nafion by Eisenberg and co-workers [20–22] showed three relaxation peaks labeled  $\alpha$ ,  $\beta$  and  $\gamma$ : the  $\alpha$  peak at around 110 °C which is independent on the water content,  $\alpha$ ,  $\beta$  peak located at around 20 °C for the dry acid form which shifted towards lower temperatures with increasing water content, and a  $\gamma$  peak at around –100 °C.

The  $\gamma$  peak is due to short-range molecular motions of the  $-\text{CF}_2-$  backbone, while the  $\beta$  peak, originally assigned to the glass transition temperature ( $T_g$ ) of the polar regions [20], was later reassigned as the glass transition of the Nafion non-ionic matrix [21]. The  $\alpha$  relaxation peak, sensitive to the ion type, degree of neutralization, and water content, was assigned to the glass transition of the polar regions [21]. It was found that the  $\alpha$  and  $\beta$  peaks shifted to higher temperatures with increasing degree of neutralization [22]. Thus, a 90% ionized Na form Nafion showed an a relaxation at around 240 °C with a shoulder ( $\beta$  relaxation) at around 140 °C, while the  $\gamma$  peak stayed at around –100 °C. The maximum of the  $\alpha$  relaxation peak, also observed in the dry acid for by Miura and Yoshida [23], seems to be shifted to higher temperatures with increasing humidity [24]. For some ionic forms of Nafion the  $\beta$  relaxation appears as a shoulder on the low temperature side of the  $\alpha$  peak [25]. Tant et al. [26] reported a transition at around 100 °C for the acid form of Nafion, but these authors did not find transitions at lower temperatures.

The ion depending  $\alpha$  and  $\beta$  relaxations were also observed by Moore and Cable [27] and the correlation of their results with molecular dynamics and NMR and SAXS experiments [28,29] allowed the authors to attribute the  $\alpha$  relaxation to the onset of long-range mobility of both the main and side chains as a result of ion-hopping processes, while the  $\beta$  relaxation was associated with the onset of segmental motions of chains within the network of electrostatically cross-linked chains.

### 1.2. Thermal properties

The motions of different parts of the Nafion structure has also been studied by thermal relaxation. Melting points (or loss of crystallinity peaks) around 207–249 °C were reported by Starkweather [30] for perfluorosulfonic acid ionomers of different molecular weights (1100–1500), obtained by DSC, but no indication is given about other thermal relaxations.

Moore and Martin [31] observed two endothermic peaks, close to 150 and 260 °C, in a DSC study of the dry  $\text{Na}^+$  form of Nafion 117 from 50 to 300 °C. They attributed these peaks to the matrix and ionic cluster transitions, respectively. The transition of the ionic cluster shifted with the ion type, from 262 °C for Na to 308 °C for Mg.

Stefanithis and Mauritz [32] reported a DSC study of Nafion in the acid form. The samples were first preheated to 130 °C for 10 min, then quenched to room temperature and the DSC scan was performed at 10 °C  $\text{min}^{-1}$  from 30 to 330 °C. Two relaxation peaks were observed; the thermal transition at 145 °C was correlated to that observed by mechanical dynamics analysis [20] and assigned to the transition of the ionic clusters, while the high temperature peak at 230 °C was attributed to the melting of the crystalline regions [30].

Similar results were obtained in other DSC studies. Thus, de Almeida and Kawano [33] found DSC endothermic peaks at 115 °C (strong) and 230 °C (weak) for the  $\text{H}^+$  form of Nafion 117 soaked in water. For the  $\text{Na}^+$  form the endothermic peaks were observed at 122 °C (strong) and 250 °C (weak). The high temperature peak in the Na form disappeared after the first run and it was not present after 3 weeks aging. The peak at low temperature also disappeared after the first run but it reappeared, shifted to higher temperatures, after an aging of few hours. The authors assigned the low temperature peak to transitions into ionic clusters instead of destruction of the aggregates. The high temperature peaks, as before, were associated with the crystalline melting of the ionomers.

Sun and Thrasher [34] also found the typical peaks due to the ionic cluster transition (around 100 °C) and the melting of the crystalline region (around 220 °C) in a DSC study of the acid form of Nafion 117 between room temperature and 600 °C.

Only three works reported DSC scans of Nafion membranes below 0 °C. Escoubes et al. [35] performed DSC runs on the acid form of Nafion 1200 in the range of temperature from –60 to 10 °C. They observed endothermic peaks at temperatures close to 0 °C due to the melting of water for membranes containing between 15% of water (100%, relative humidities, RH), but at lower water content the peak was very broad and shifted to lower temperature and no peaks were found for water content below 8% (less than 50% RH).

Kawano and co-workers [36] performed DSC of Nafion 117 in the  $\text{Mg}^{2+}$ ,  $\text{Ca}^{2+}$ ,  $\text{Sr}^{2+}$ , and  $\text{Ba}^{2+}$  forms in the temperature range –50 to 350 °C at 10 °C  $\text{min}^{-1}$ . They observed two kinds of transitions: one in the range –30 to 40 °C associated to the water melting and other in the range 100 to 200 °C interpreted as a loss of water of the ionic cluster, accompanied by a polymer contraction. The low temperature transitions were not observed

during the second run, probably because there was no time for water reabsorption.

In order to obtain information on the amount of freezable water, Asaka et al. [37] performed DSC studies of Nafion 117 in the temperature range  $-35$  to  $20$  °C at  $1$  °C  $\text{min}^{-1}$ . The heating curves presented two endothermic peaks of melting of the freezable pore water: one broad peak at around  $-4$  °C and a sharp peak close to  $0$  °C. The cooling curves presented an exothermic peak due to the freezing of water previously supercooled in the pores. The analysis of the freezable water for different counterions indicates that the  $\text{Li}^+$  form has 16% of freezable water, the  $\text{Na}^+$  form 21% and other cations ( $\text{K}^+$ ,  $\text{Cs}^+$ ,  $\text{Ca}^{2+}$ ,  $\text{Mg}^{2+}$ ,  $\text{Ba}^{2+}$ ,  $(\text{CH}_3)_4\text{N}^+$ , and  $(\text{CH}_3\text{CH}_2)_4\text{N}^+$ ) between 10 and 14%. For tetrapropyl and tetrabutyl ammonium ions the amount of freezable water decreased to less than 2%.

It is clear from this summary that thermal studies of Nafion membranes are scarce in the low temperature region and no evidence is reported so far of the peak defined as  $\gamma$ , observed by mechanical studies at temperatures about  $-100$  °C. On the other hand, any systematic study is available on the effect of the water content on the thermal relaxation of Nafion membranes.

The purpose of this work is to characterize low temperature thermal transitions of Nafion 117 membranes in water and methanol–water mixtures and assess the amount of freezable water in these membranes as a function of the water content.

## 2. Experimental

### 2.1. Materials

The Nafion 117 membrane (DuPont Inc.) has an equivalent weight of 1100, or an ion-exchange capacity of  $0.91$  meq  $\text{g}^{-1}$ , and a thickness of  $178$   $\mu\text{m}$ . All the Nafion membranes used in this study were cleaned and converted into the acid form using a standard procedure as follows: the membranes were treated serially in hydrogen peroxide solution (3 wt.%) to eliminate organic impurities, water, sulfuric acid ( $1$  mol  $\text{dm}^{-3}$ ) to protonate the membrane, and finally soaked with water at  $80$  °C for 1 h. Portions of pretreated membrane were immersed for 18 h in  $1$  M NaCl aqueous solution in order to exchange the counterion and convert the membrane into the  $\text{Na}^+$  form, and then washed with water to remove excess electrolyte. The pretreated membranes were then cut into discs of  $5$  mm and equilibrated at different relative humidities or immersed in water or in methanol–water solutions. The membranes immersed in water or in methanol–water were wiped gently with paper to remove superficial solution before DSC analysis.

Dry membranes in the acid forms were obtained by two methods: (i) by equilibrating the membrane with  $\text{P}_2\text{O}_5$  by several days; (ii) by heating the membrane at  $105$  °C overnight.

Analytical grade methanol (Merck) and milli-Q water were used to prepare the solutions.

### 2.2. Thermophysical properties

The glass transition temperatures ( $T_g$ ), the reversible change of specific heat capacity at the glass transition ( $\Delta C_p$ ), crystal-

lization and melting temperatures ( $T_c$  and  $T_m$ , respectively) and heats of crystallization ( $\Delta H_c$ ) and fusion ( $\Delta H_f$ ) were determined from the peak areas by differential scanning calorimetry (DSC) using a Mettler 822 and STARe Thermal Analysis System version 6.1 software (Mettler Toledo AG, Switzerland).

Glass transitions were recorded as the onset temperature of the discontinuities in the curves of heat-flow versus temperature (change in heat capacity); crystallization and melting temperatures ( $T_c$  and  $T_m$ , respectively) were taken to be the onset temperatures of the exothermic and endothermic changes, respectively. The instrument was calibrated using standard compounds (indium, zinc and lead) of defined melting point and heat of melting.

All measurements were made with 8–20 mg sample mass, at a scanning rate of  $10$  °C  $\text{min}^{-1}$  using hermetically sealed aluminium pans of  $40$   $\mu\text{L}$  inner volume (Mettler) and an empty pan was used as a reference. Each sample was cooled and maintained isothermal at  $-145$  °C during 3 min previously to the dynamic DSC runs performed from  $-145$  to  $25$  °C at a scanning rate of  $10$  °C  $\text{min}^{-1}$ . Reported data are the average of three determinations.

## 3. Results and discussion

### 3.1. High temperature DSC scans of dry and hydrated Nafion 117

Fig. 1a and b show the typical DSC scans of Nafion 117 membranes above room temperatures. The scans in Fig. 1a correspond to membranes dried at room temperature and at  $105$  °C. It is observed that the membrane dried at room temperature presents a peak around  $150$  °C (in other sample, not shown here, the peaks appeared at  $190$  °C), while in the sample dried at  $105$  °C the peak is weaker. This could be due to fact that water is still present in the ionic cluster after drying, because in both cases the peaks disappeared in the second scan, recorded after keeping the membranes in an anhydrous atmosphere for 2 weeks. The differences observed with the results by de Almeida and Kawano [33] are due to the fact that these authors allowed the re-absorption of water during 3 weeks after the first scan.

A high temperature relaxation is also observed in the dry samples (Fig. 1a) above  $200$  °C, which can be attributed to melting of the crystalline domains [30]. This relaxation is also observed in the second scan (although with lower intensity), probably because the melting of the crystalline regions requires heating above  $280$  °C [33].

The DSC scans for samples dried at room temperature and at  $105$  °C and then equilibrated with water at 100% RH either, by immersion in liquid water or by exposing them to saturated water vapor, are shown in Fig. 1b. Again, the first run show a peak around  $100$  °C that is stronger in the case of membranes equilibrated with water vapor. The peaks are absent in the second runs performed 2 weeks later. The high temperature transition is much weaker in samples equilibrated with water, as shown in Fig. 1b (note the scale difference with Fig. 1a). This result is expected taking into account the plasticizer effect of water on the polymer, that is, the degree of crystallinity of the sample decrease

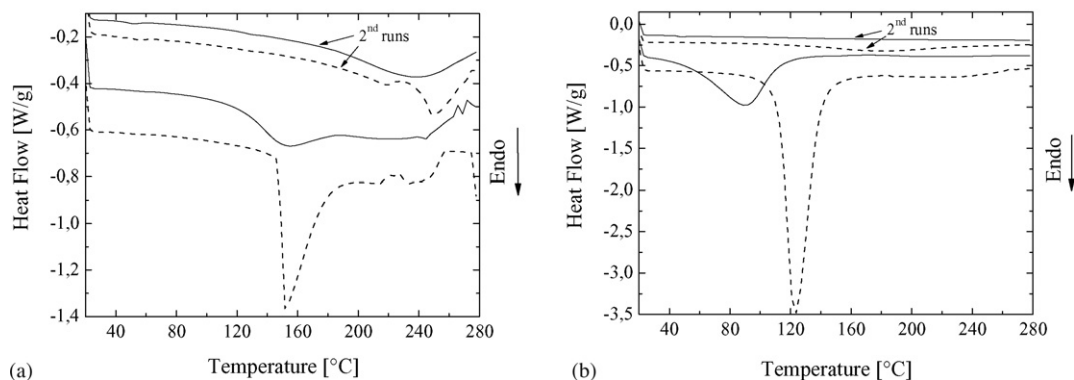


Fig. 1. DSC curves of Nafion 117 membranes ( $H^+$  form) at temperatures above room temperature: (a) dry Nafion; (b) Nafion equilibrated with water vapor. The solid and dashed lines correspond to membranes dried at 105 °C and room temperature, respectively. The second runs were performed 2 weeks after than the first ones.

as increasing water content in the membrane as suggested by the analysis of previous results [32,33].

The onset of the water desorption from the ionic clusters peaks are different for the dried (Fig. 1a) and water equilibrated (Fig. 1b) samples, and different onset is also observed for the water equilibrated sample depending on the drying temperature. This behavior is due to both, the different interaction of water with the ionomeric matrix, which in turns depends on the water content, and the thermal history of the sample. The higher desorption temperature for the dried samples is an indication of stronger interaction of the remnant water with sulphonic groups and counterions in the membrane.

In summary, there are two thermal relaxations peaks above room temperature. The first one, which is observed in the range 100–150 °C, corresponds to the desorption of water from the ionic cluster and most of the previous authors called it the glass transition temperature of the ionic cluster. However we prefer to attribute this peak to the desorption of water from the ionic cluster, that it does not means that a glass transition is taking place in this region. Since the energy involved in this process depends on the interaction energy of water with the ionic species, the temperature of the peak will change with the type of counterion and the water content in the membrane, as already noted in the literature [33,36].

### 3.2. Low temperature DSC scans of Nafion 117 equilibrated with water

The glass transition temperature of Nafion backbone should be in the subzero region, coincidentally with the  $\gamma$  peak of the dynamics mechanical studies [20]. In this section we analyze the low temperature portion of the DSC scans for Nafion samples containing water, while in the next section we will deal with Nafion membranes containing water–methanol mixtures.

The DSC scans of Nafion 117 membranes (H form) equilibrated at different RH are shown in Fig. 2a., and the characteristic temperatures, heat capacity changes at  $T_g$  and enthalpy changes are summarized in Table 1. The thermogram of the Na form was included for comparative purposes. The samples at 0 and 44% RH did not present the peak corresponding to ice melting, observed in the samples at RH values between 84 and 100%.

In addition, all samples in Fig. 2a, except for the one in the  $Na^+$  form, showed a weak transition between  $-108$  and  $-130$  °C which is better observed in Fig. 2b. These thermal transitions could be associated with the glass transition of the Nafion matrix, that is, with the motion of the Nafion backbone, and would correspond to the  $\gamma$  peak observed by Kyu et al. [22] using dynamics mechanical techniques. Our findings are the first evidence of such a transition observed by thermal relaxation and the onset

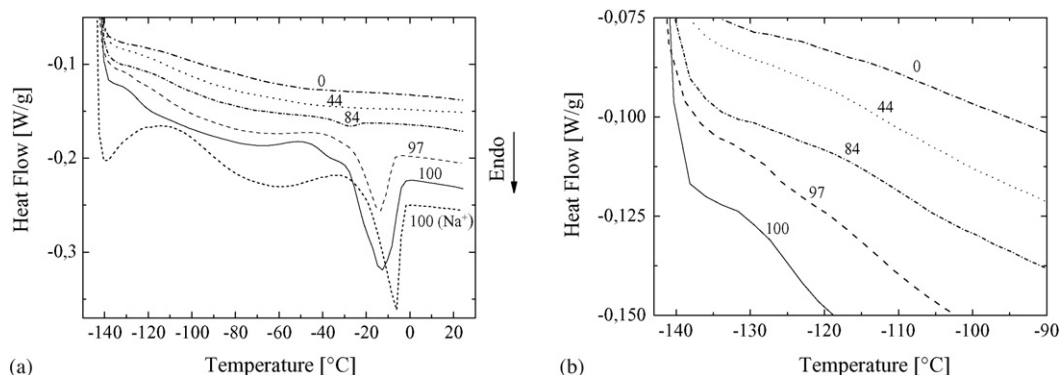


Fig. 2. DSC curves of Nafion 117 membranes ( $H^+$  form) equilibrated at different % RH (indicated on the curves) and of Nafion 117 in the  $Na^+$  form at 100% RH. Scan rate, 10 °C  $min^{-1}$ . (a) Full scale; (b) Zoom of the glass transition region.

Table 1

Glass transition temperature ( $T_g$ ), reversible change of specific heat capacity at  $T_g$  ( $\Delta C_p$ ), crystallization and melting temperatures ( $T_c$  and  $T_m$ , respectively), heats of crystallization ( $\Delta H_c$ ) and fusion ( $\Delta H_f$ ) per gram of Nafion sample, water solubility ( $N$ ) in  $\text{g g}^{-1}$  (dry Nafion) and freezable water content ( $W_f$ ) in Nafion® 117, for the different percentages of relative humidity (RH) and for Nafion in the  $\text{Na}^+$  form at 100% RH

Water (RH)	$T_g$ ( $^{\circ}\text{C}$ )	$T_c$ ( $^{\circ}\text{C}$ )	$T_m$ ( $^{\circ}\text{C}$ )	$\Delta C_p$ ( $\text{J g}^{-1} \text{ } ^{\circ}\text{C}^{-1}$ )	$\Delta H_c$ ( $\text{J g}^{-1}$ )	$\Delta H_f$ ( $\text{J g}^{-1}$ )	$\Delta H_c/\Delta H_f$ (%)	$N$ ( $\text{g g}^{-1}$ , dry)	$W_f$ (%)
0	−108	–	–	0.117	–	–	–	0	–
44	−122	–	–	0.251	–	–	–	0.050	–
84	−125	−56	−35	0.258	0.08	−0.33	24	0.142	1
97	−127	−61	−26	0.214	0.87	−4.21	21	0.205	8
100	−132	−67	−25	0.170	2.04	−13.8	15	0.220	23
100 ( $\text{Na}^+$ )	–	−55	−23	–	3.11	−7.19	43	0.220 <sup>a</sup>	12

<sup>a</sup> The same water uptake than in the  $\text{H}^+$  form was assumed.

of the endothermic  $C_p$  change (characteristic of a glass transition) slightly decreased with increasing water content (Table 1), indicating a certain plasticizing effect of water on the amorphous regions of Nafion.

The heat capacity change ( $\Delta C_p$ ) is considered the most important of all the observable thermodynamic discontinuities during a glass transition because of its relation to the Kauzmann vanishing excess entropy paradox [38,39]. It reflects the access of the system to additional (configurational) degrees of freedom in the diffusive liquid state above the glass transition, and, as the heat capacity of the liquid is higher than the heat capacity of the glass,  $\Delta C_p$  should always be positive. The values shown in Table 1 for Nafion with different degrees of hydration, lied in an intermediate range between those for polyols and those for several synthetic polymers [39,40].

It is interesting to compare the value of  $T_g$  of dry Nafion with those reported for polytetrafluoroethylene which is the non-ionic polymer related to Nafion. The reported  $T_g$  value for PTFE is  $-113^{\circ}\text{C}$  [41], that is surprisingly close to the dry Nafion value obtained in this work ( $T_g = -108^{\circ}\text{C}$ ). This reinforces the idea that the observed glass transition temperature is related to the coordinated molecular motion of a limited number (10–50) chain atoms, in such a way that the ionic clusters have a small effect on the onset of this transition.

At and above 84% RH, an endothermic peak appeared, whose onset temperature was between  $-25$  and  $-35^{\circ}\text{C}$ , this peak can be attributed to the melting of freezable water. At 97 and 100% RH, a small exothermal peak could also be observed at temperatures of  $-61$  and  $-67^{\circ}\text{C}$  (onset), respectively, which corresponds to the crystallization of freezable water that was supercooled during cooling at  $-145^{\circ}\text{C}$ . The DSC curves of Fig. 2a are heating curves and the crystallization exothermal peak corresponds to water that did not crystallize during cooling, i.e. water that was supercooled. The Nafion sample in the  $\text{Na}^+$  form presented a comparatively larger exothermal peak area at 100% RH, when compared to the rest of the samples and this is evidenced by the factor  $\Delta H_c/\Delta H_f$  in Table 1.

As proposed by Gierke et al. [42], Nafion is considered to have a so-called ion-cluster structure, that is, spherical ion-water clusters of ca. 4 nm diameter connected by 1 nm diameter channels. In the DSC curves shown in Fig. 2a, a lower melting temperature of water in the membrane was observed in comparison to bulk water. On the basis of an ion-cluster structure of Nafion mentioned above, this decrease in the melting temperature of water

can be explained considering the size of the critical nuclei for solidification: when the hydrophilic cluster or pores of Nafion are smaller than the critical nuclei for ice formation, a depression in solidification- and melting-temperature occurs. In addition, freezable water interacting in the ion-cluster structure of Nafion may also contribute to the depression of the melting temperature due to polymer-water interaction [37]. It can be then considered that the exothermic and endothermic peaks are due to the freezable pore water in the hydrophilic cluster or channel of the Nafion. On the basis of the temperature of the melting peak, no bulk-like water was observed in Fig. 2a.

Strongly hydrated membranes ( $>84\%$  RH) may contain three different types of water associated with Nafion and can be characterized by DSC measurements: (1) non-freezable pore water, bound to the sulfonic groups, located in the ionic clusters; (2) freezable pore bound water, weakly bound to the ionic groups and the polymer matrix; and (3) free water that is not intimately bound to the polymer chain and behaves like bulk water.

Since the endothermic peaks in the DSC curves are attributed to the freezable pore water, the freezable pore water content ( $W_f$ ) in the Nafion membrane can be estimated from the peak area. The value of the melting enthalpy of ice I,  $333.8 \text{ J g}^{-1}$  was employed to estimate freezable pore water content [43]. The total water content of the membranes for each relative humidity was obtained from the sorption isotherm curve of water in Nafion [6], and reported in Table 1. The percentage of freezable pore water (%  $W_f$ ) shown in Table 1 was then obtained as the ratio of the freezable water to the total water content.

### 3.3. Low temperature DSC scans of Nafion 117 equilibrated with water–methanol

Fig. 3a corresponds to DSC curves of water–methanol mixtures 25 and 50% wt. methanol and Fig. 3b shows the DSC curves of the Nafion samples ( $\text{H}^+$  form) equilibrated in methanol–water solutions, from 25 to 100% wt. methanol.

It is interesting to note that the endothermic peaks corresponding to the melting of ice in the water–methanol samples (Fig. 3a) were in agreement with those previously reported in the phase diagram of the binary mixture [44]: the melting temperature of the water–methanol mixture decreases from  $-27$  to  $50^{\circ}\text{C}$  when methanol concentration increased from 25 to 50%. In the Nafion samples (Fig. 3b), however, the peaks shifted only slightly towards lower temperatures as the methanol concen-

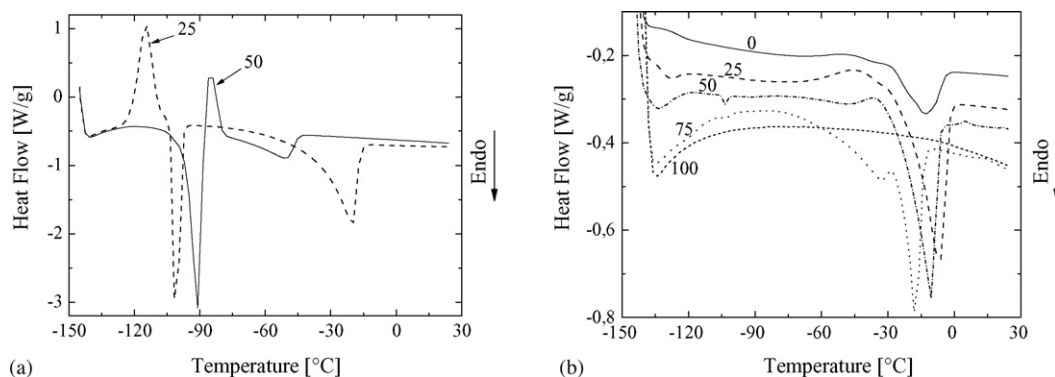


Fig. 3. DSC curves of: (a) methanol–water solutions; (b) Nafion 117 membranes equilibrated in methanol–water solutions. Scan rate,  $10^{\circ}\text{C min}^{-1}$ . The numbers indicate the percentage (w/w) of methanol in the mixture.

Table 2  
Water crystallization and melting temperatures ( $T_c$  and  $T_m$ , respectively), heats of crystallization ( $\Delta H_c$ ) and fusion ( $\Delta H_f$ ), and freezable water content ( $W_f$ ) in Nafion<sup>®</sup> 117 with different methanol–water compositions

CH <sub>3</sub> OH (wt.%)	$T_c$ (°C)	$T_m$ (°C)	$\Delta H_c$ (J g <sup>-1</sup> )	$\Delta H_f$ (J g <sup>-1</sup> )	$\Delta H_c/\Delta H_f$ (%)	$N$	$W_f$ (%)
25	-59	-13	4.59	-28.8	16	0.165	61
50	-50	-18	3.19	-26.2	12	0.110	65
75	-32	-23	1.12	-11.4	9.8	0.055	65

tration increased from 25 to 75% wt. The peaks observed at around  $-103^{\circ}\text{C}$  for the water–methanol mixtures, also appreciable in the Nafion samples, correspond to the melting of the solid methanol hydrated ( $\text{CH}_3\text{OH}\cdot 2\text{H}_2\text{O}$ ) first formed from the supercooled liquid on cooling [44].

It is to be noted that the water crystallization and melting peak areas in these methanol–water curves were larger than those obtained for the samples equilibrated in pure water. In order to estimate the amount of freezable water, the solubility of water in the samples at the different water–methanol compositions were calculated assuming that the composition in the membrane was identical to that of the binary liquid mixture were it was immersed, as pointed out by Ren et al. [5].

As shown in Table 2, the percentage of freezable water (61–65%) was practically independent on the amount of methanol in the membrane (in the studied concentration range) and it was much larger than that observed in membranes equilibrated in pure water (23%). Since the solubility of water and methanol, expressed in mol per gram of dry membrane, are 0.012 and 0.015, respectively [6], it is not expected that the difference in the amount of freezable water be a result of water segregation in the ionic clusters. It is plausible that the difference might be originated in the lack of freezing of methanol during the sample cooling. Thus, supercooled methanol could replace water in the solvation of the ionic groups which in turns lead to an increase in the amount of freezable water in the membrane. This is supported by the lack of the melting peak corresponding to the methanol dihydrate, as shown in Fig. 3b

In Nafion samples immersed in methanol–water solutions a transition attributable to a glass transition seemed to occur below  $130^{\circ}\text{C}$  but it could not be assessed, since its location was close to the lower experimentally accessible limit of the temperature scale.

#### 4. Conclusions

Low-temperature transition of Nafion were analyzed by DSC, and the evidence of thermal relaxations were in agreement with previously analyzed mechanical relaxations.

In the dry Nafion (acid form) samples, a thermal transition was observed at  $-108^{\circ}\text{C}$ , which was attributable to a glass transition. When increasing the relative humidity to which the samples were exposed, this thermal transition shifted to lower temperatures, indicating that water has a slight plasticizing effect on the Nafion membrane, which is not so dramatic as that observed for biopolymers (it is to be noted that the glass transitions of biopolymers decrease from about  $250$  to  $0^{\circ}\text{C}$  in the same range of RH). The presence of freezable water was detected when the samples were exposed at and above 84% RH. The Nafion sample in the  $\text{Na}^+$  form allowed a larger amount of water to remain in non-crystalline (supercooled) state.

The presence of methanol increased the amount of freezable water probably due to the supercooling of methanol or methanol dihydrate upon cooling, which could lead to the replace of water by methanol in the solvation of ionic groups on the matrix.

The freezing of water in Nafion containing water–methanol takes place at temperatures in the range of  $-10$  to  $-20^{\circ}\text{C}$ , being relevant to the operation of direct methanol PEM fuel cells in low temperature environments. The amount of freezable water could be the criteria for choosing membranes for this type of fuel cells, beyond the methanol permeation characteristics.

#### Acknowledgments

The authors thank financial support from Agencia Nacional de Promoción Científica y Tecnológica (PICT 06-13917), from CNEA (Project P5 PID 36-3) and from University of Buenos

Aires (Project X-220/84/98). FNP thanks doctoral fellowships from Consejo Nacional de Investigaciones Científicas y Técnicas (CONICET).

## References

- [1] D.J. Connolly, W.F. Gresham, US Patent 3,282,875, 1966.
- [2] M. Doyle, G. Rajendran, in: W. Vielstich, H.A. Gasteiger, A. Lamm (Eds.), Handbook of Fuel Cells-Fundamentals, Technology and Applications, 3, John Wiley & Sons, New York, 2003, p. 351.
- [3] T.A. Zawodzinski Jr., C. Derouin, S. Radzinski, R.J. Sherman, V.T. Smith, T.E. Springer, S. Gottesfeld, J. Electrochem. Soc. 140 (1993) 1041.
- [4] J.T. Hinatsu, M. Mizuhata, H. Talçkenaka, J. Electrochem. Soc. 141 (1994) 1493.
- [5] X. Ren, T.E. Springer, S. Gottesfeld, J. Electrochem. Soc. 147 (2000) 92.
- [6] D. Rivin, C.E. Kendrick, P.W. Gibson, N.S. Schneider, Polymer 42 (2001) 623.
- [7] H.L. Yeager, A. Steck, J. Electrochem. Soc. 128 (1981) 1880.
- [8] T. Okada, G. Xie, O. Gorseth, S. Kjelstrup, N. Nakamura, T. Arimura, Electrochim. Acta 43 (1998) 3741.
- [9] V. Tricoli, J. Electrochem. Soc. 145 (1998) 3798.
- [10] V. Tricoli, N. Carretta, M. Bartolozzi, J. Electrochem. Soc. 147 (2000) 1286.
- [11] S.J. Paddison, R. Paul, Phys. Chem. Chem. Phys. 4 (2002) 1158.
- [12] P. Dimitrova, K.A. Friedrich, B. Vogt, U. Stimming, J. Electroanal. Chem. 532 (2002) 75.
- [13] T.A. Zawodzinski Jr., M. Neeman, L.O. Sillerud, S. Gottesfeld, J. Phys. Chem. 95 (1991) 6040.
- [14] T.F. Fuller, J. Newman, J. Electrochem. Soc. 139 (1992) 1332.
- [15] X. Ren, W. Henderson, S. Gottesfeld, J. Electrochem. Soc. 144 (1997) L267.
- [16] C.M. Gates, J. Newman, AIChE J. 46 (2000) 2076.
- [17] P.S. Kauranen, E. Skou, J. Appl. Electrochem. 26 (1996) 909.
- [18] X. Ren, T.E. Springer, T.A. Zawodzinski, S. Gottesfeld, J. Electrochem. Soc. 147 (2000) 466.
- [19] K.A. Mauritz, R.B. Moore, Chem. Rev. 104 (2004) 4535.
- [20] S.C. Yeo, A.J. Eisenberg, J. Appl. Polym. Sci. 21 (1997) 875.
- [21] T. Kyu, A. Eisenberg, Perfluorinated ionomer membranes, in: A. Eisenberg, H.L. Yeager (Eds.), Proceedings of the Am. Chem. Soc. Symposium Series 180, Washington, DC, 1982, p. 79, Chapter 6.
- [22] T. Kyu, M. Hashiyama, A. Eisenberg, A. Can. J. Chem. 61 (1983) 680.
- [23] Y. Miura, H. Yoshida, Thermochim. Acta 163 (1990) 161.
- [24] F. Bauer, S. Denneler, M. Willert-Porada, J. Polym. Sci. B, Polym. Phys. 43 (2005) 786.
- [25] K.M. Cable, Ph.D. dissertation, University of Southern Mississippi, 1996.
- [26] M.R. Tant, K.P. Darst, K.D. Lee, C.W. Martin, Multiphase polymers: blends and ionomers, in: L.A. Utracki, R.A. Weiss (Eds.), Proceedings of the Am. Chem. Soc. Symposium Series 180, Washington, DC, 1989, p. 370, Chapter 15.
- [27] R.B. Moore, K.M. Cable, Polym. Preprint (Am. Chem. Soc. Div. Polym. Chem.) 38 (1997) 272.
- [28] K.A. Page, R.B. Moore, Polym. Preprint (Am. Chem. Soc. Div. Polym. Chem.) 44 (2003) 1144.
- [29] F.A. Landis, R.B. Moore, K.A. Page, C.C. Han, Polym. Mater. Sci. Eng. (Am. Chem. Soc. Div. Polym. Mater. Sci. Eng.) 87 (2002) 121.
- [30] H.W. Starkweather, Macromolecules 15 (1982) 320.
- [31] R.B. Moore, C.R. Martin, Macromolecules 21 (1988) 1334.
- [32] I.D. Stefanithis, K.A. Mauritz, Macromolecules 23 (1990) 2397.
- [33] S.H. de Almeida, Y. Kawano, J. Therm. Anal. Cal. 58 (1999) 569.
- [34] L.Y. Sun, J.S. Thrasher, Polym. Degrad. Stab. 89 (2005) 43.
- [35] M. Escoubes, M. Pineri, E. Robens, Thermochim. Acta 82 (1984) 149.
- [36] L. Gomes Lage, P. Gomes Delgado, Y. Kawano, Eur. Polym. J. 40 (2004) 1309.
- [37] K. Asaka, N. Fujiwara, K. Oguro, K. Onishi, S. Sewa, J. Electroanal. Chem. 505 (2001) 24.
- [38] W. Kauzmann, Chem. Rev. 43 (1948) 219.
- [39] C.A. Angell, Pure Appl. Chem. 63 (1991) 1387.
- [40] B. Wunderlich, Thermochim. Acta 432 (2005) 127.
- [41] L.H. Sperling, Introduction to the Physical Polymer Science, John Wiley & Sons, New York, 1992, p. 337, Chapter 8, reported as a personal communication from H. Starkweather, du Pont de Nemours and Company.
- [42] T.D. Gierke, G.E. Munn, F.C. Wilson, J. Polym. Sci., Polym. Phys. 19 (1981) 1687.
- [43] G. Xie, T. Okada, Electrochim. Acta 41 (1996) 1569.
- [44] K. Takaizumi, T. Wakabayashi, J. Solution Chem. 26 (1997) 927.